Project 2: Polarization of Light

Gianfranco Grillo

September 27th, 2017

Abstract

We present the results of a series of five experiments designed to investigate different aspects of the polarization of light. In the first experiment, we perform a verification of Malus's Law and find the extinction ratio between two identical polarizers. Our results are consistent with Malus's Law, and we calculate the extinction ratio as x, which is close to the nominal value. The second experiment measures the index of refraction n of a glass prism by finding its Brewster's angle, obtaining a value of $n = 1.46 \pm 0.05$. In the third experiment, we measure the reflectance coefficient of a blackened flat in two different ways, one by fitting a curve according to Fresnel's equations, and another by finding the azimuthal angle. We find general agreement between the two methods. In the fourth experiment, we qualitatively examine the polarization of light by scattering. Finally, we study the effects of birefringent materials on incident light, and determine the phase shift ϕ introduced by an overhead transparency on linearly polarized light. We find that $\phi = 70 \pm 10°$.

1 Introduction

According to classical electromagnetism, light consists in electromagnetic waves of a particular frequency that propagate in a direction perpendicular to the oscillations of the electric field and the magnetic field. As long as they are perpendicular with respect to each other and the direction of propagation, the electric and magnetic fields can oscillate in an arbitrary orientation. The geometrical characteristics of this orientation are known as the wave's polarization. Monochromatic polarized light traveling in an arbitrarily defined z-direction can be described in a straightforward manner in terms of the amplitudes of the x- and y-components of their electric fields, as well as the phase difference between them. In this project, we use a monochromatic laser beam of wavelength 632.8 nm and perform a series of measurements that can be successfully modeled under this framework.

We perform the data analysis using Python and the associated library SciPy ([1]) and Uncertainty package ([2]).

2 Theoretical background

2.1 Electromagnetic waves

The wave equations in vacuum for the electric field $\vec{E}$ and the magnetic field $\vec{B}$ follow from Maxwell's equations and are given by

$$\nabla^2 \vec{E} = \epsilon_0 \mu_0 \frac{\partial^2 \vec{E}}{\partial t^2} \tag{1}$$

$$\nabla^2 \vec{B} = \epsilon_0 \mu_0 \frac{\partial^2 \vec{B}}{\partial t^2} \tag{2}$$

where ϵ_0 and μ_0 are the permittivity and permeability of free space, respectively. Faraday's Law states that

$$\vec{\nabla} \times \vec{E} = -\frac{\partial \vec{B}}{\partial t} \tag{3}$$

Following the derivation in [3], we can consider the case of a monochromatic plane wave of linear polarization moving in the z-direction, where the electric and magnetic fields are given by

$$\tilde{E} = \tilde{E}_0 e^{i(kz-\omega t)} \tag{4}$$

$$\tilde{B} = \tilde{B}_0 e^{i(kz-\omega t)} \tag{5}$$

Gauss's Law for electric and magnetic fields in free space requires that

$$\vec{\nabla} \cdot \vec{B} = \vec{\nabla} \cdot \vec{E} = 0 \tag{6}$$

which implies that both fields are transverse to the direction of propagation of the wave, since

$$(\vec{E}_0)_z = (\vec{B}_0)_z = 0 \tag{7}$$

Moreover, equation (3) forces the electric and magnetic fields to be perpendicular to each other, since (3) requires that

$$-k(\tilde{E}_0)_y = \omega(\tilde{B}_0)_x,\ k(\tilde{E}_0)_x = \omega(\tilde{B}_0)_y \tag{8}$$

This can also be expressed as

$$\tilde{B}_0 = \frac{k}{\omega}(\hat{z} \times \tilde{E}_0) \tag{9}$$

In linear, non-absorbing media with no free charge or free current, this relationship also holds, since equation (6) is still true, and the only change in the other equations is that the constants in Faraday's law change from ϵ_0 and μ_o to the corresponding permittivity and permeability of the specific medium in question, ϵ and μ. Thus the velocity of the wave changes, but not their transverse quality or the characteristic that the electric and magnetic fields are perpendicular to each other.

2.2 Polarization by a plastic film

One of the properties that describes electromagnetic waves is their polarization, which is related to the geometrical orientation of their electric fields. The orientation of the electric field of an electromagnetic wave traveling in the +z-direction can be described in terms of the relationships between the amplitudes and phases of the electric field's x- and y-components. We say that light is linearly polarized when

one of the components of the electric field is equal to zero, and thus the electric field oscillates in only one axis.

Linear polarization can be achieved by means of a thin plastic film made of polymer chains covered with iodine. Iodine is a light absorbing element, and the plastic film is manufactured in such a way that the polymer chains align in a particular direction. Randomly polarized light incident in such a film becomes linearly polarized, as only the component of the electric field perpendicular to the direction of the film's polymer chains is transmitted by the film. The iodine covering the polymer chains preferentially absorbs the light incident parallel to it, as its electrons are able to oscillate freely along that axis. The radiation emitted due to the oscillations of these electrons is 180° out of phase with respect to the incident radiation, which means that very little light gets transmitted with its field oscillating in that direction. The only direction in which the electrons cannot oscillate at all is perpendicular to the direction of the polymer chains, so the component of the electric field along this axis is the only one that is transmitted by the film.

2.3 Malus's Law

An optical system composed of two linear polarizers will transmit a certain amount of light that depends on the relative orientations of the axes of the two constituent polarizers. The precise relationship between the transmitted intensity I and the angle between the axes of the polarizers θ is known as Malus's Law, and is given by

$$I(\theta) = I_0 \cos^2 \theta \tag{10}$$

where I_0 corresponds to the intensity of the light emerging from the first polarizer. The obvious consequences of this relationship is that maximum transmission occurs when $\theta = 0°$, that is, when the two polarizer axes are aligned with each other, whereas minimum transmission occurs when $\theta = 90°$, which corresponds to the configuration in which the axes of transmission of both polarizers are perpendicular to each other. This law should hold exactly for the case of two ideal polarizers which transmit all the light incident along their transmission axis and block all other light. In practice, however, some of the light that is not parallel to the transmission axis is allowed to go through, and some of the light parallel to the transmission axis is blocked. A measure of deviation from ideal is the extinction ratio r_e, given by

$$r_e = \frac{I_{min}}{I_{max}} \tag{11}$$

where I_{min} and I_{max} correspond to the minimum intensity and maximum intensities emerging from the system, respectively.

2.4 Fresnel's equations and Brewster's angle

The electric field of an electromagnetic wave incident on a surface can be conveniently expressed in terms of its components parallel ($E_\parallel$) and perpendicular ($E_\perp$) to the plane of incidence. The Fresnel equations relate the magnitude of the reflected fields to that of the incident fields for each of the components, and are given in [4] as

$$r_\parallel = \frac{E_{\parallel_r}}{E_{\parallel_i}} = \frac{\tan(\theta_i - \theta_t)}{\tan(\theta_i + \theta_t)} \tag{12}$$

$$r_\perp = \frac{E_{\perp_r}}{E_{\perp_i}} = -\frac{\sin(\theta_i - \theta_t)}{\sin(\theta_i + \theta_t)} \tag{13}$$

These ratios are also known as the reflection coefficients. The incident wave becomes completely polarized when $r_{\parallel}$ vanishes, which occurs when its denominator $\tan(\theta_i + \theta_t) \to \infty$, that is, when $\theta_i + \theta_t = 90°$. Snell's Law indicates that for an air/dielectric interface,

$$n \sin\theta_t = \sin\theta_i = \sin(90° - \theta_t) = \cos\theta_t \tag{14}$$

Solving for θ_t gives the transmission angle that results in completely polarized light, also known as Brewster's angle θ_b, in honor of Sir David Brewster, who first discovered it in 1815.

$$\theta_b = \arctan(n) \tag{15}$$

We will calculate the refractive index of a glass prism in experiment 2 by means of this equation.

Using trigonometric identities and Snell's Law, it is possible to rewrite (12) and (13) strictly in terms of θ_i and n,

$$r_{\parallel} = \frac{n^2 \cos\theta_i - \sqrt{n^2 - \sin^2\theta_i}}{n^2 \cos\theta_i + \sqrt{n^2 - \sin^2\theta_i}} \tag{16}$$

$$r_{\perp} = \frac{\cos\theta_i - \sqrt{n^2 - \sin^2\theta_i}}{\cos\theta_i + \sqrt{n^2 - \sin^2\theta_i}} \tag{17}$$

Experiment 3 of this project will verify these equations by comparing the incident intensities of light alternatively polarized along the plane of incidence and perpendicular to the plane of incidence to the reflected intensities, as a function of θ_i. The ratio between the reflected intensity and the incident intensity corresponds to the square of the ratio of the reflected electric field and the incident electric field. That is$R_{\parallel} = r_{\parallel}^2$, and $R_{\perp} = r_{\perp}^2$, so our measurements should be described by the square of equations (16) and (17).

2.5 Polarization and scattering

Randomly polarized light incident on a group of molecules causes the molecules to start oscillating parallel to the direction of the light's electric field's oscillations. Because the light is unpolarized, the direction of oscillation will change with time in a practically random way, but it will always be perpendicular to the direction of the light's propagation. This means that molecules will oscillate perpendicularly to the direction of propagation. As explained in section 2.2, as the molecules oscillate, they reradiate light in all directions except for that of their axis of oscillation, and the reradiated light will be out of phase with respect to the incident light, which will result in the light becoming polarized. In practice, this means that the reradiated light emerging from a direction normal to that of the propagation of the incident light beam will be completely linearly polarized, and the reradiated light emerging in the same direction of the incident beam will emerge randomly polarized. A more detailed explanation of this phenomenon can be found in [5]. The light reradiated in directions that are neither normal nor perpendicular to the direction of propagation will be partially polarized. Experiment 4 qualitatively verifies these concepts.

2.6 Birefringence

Birefringence corresponds to the phenomenon in which the components of a beam's electric field undergo a relative phase shift as they pass through a material, because not all the beam's light is able to travel at the same speed within the material. Depending on the geometrical orientation of the

beam's constituent electric fields, the velocity at which parts of the beam travel is different from that of other parts, because a birefringent material has more than one refractive index. In experiment 5, we will examine the properties of a uniaxial birefringent material, for which one of its axes has a different refractive index than the other two.

The first setup in that experiment will involve placing a quarter wave plate in between two polarizers, with respect to the orientation of a laser beam's propagation. Linearly polarized light passing through a quarter wave plate becomes circularly polarized because the quarter wave plate introduces a phase shift of 45° between the x- and y-components of the incident electric field. Crossing the first polarizer with the second polarizer (which in this context is referred to as an analyzer), and introducing the quarter wave plate in between them with its fast axis at an angle of θ with respect to the horizontal axis of the system, and rotating the system in such a way that the transmission axis of the first polarizer points in the y-direction, implies that the transmitted components of the electric field are proportional to

$$\begin{aligned}
\begin{bmatrix} E_{t_x} \\ E_{t_y} \end{bmatrix} &\propto e^{-\frac{i\pi}{4}} \begin{bmatrix} 1 & 0 \\ 0 & 0 \end{bmatrix} \begin{bmatrix} \cos^2\theta + i\sin^2\theta & (1-i)\sin\theta\cos\theta \\ (1-i)\sin\theta\cos\theta & \sin^2\theta + i\cos^2\theta \end{bmatrix} \begin{bmatrix} 0 \\ 1 \end{bmatrix} && (18) \\
&\propto e^{-\frac{i\pi}{4}} \begin{bmatrix} 1 & 0 \\ 0 & 0 \end{bmatrix} \begin{bmatrix} (1-i)\sin\theta\cos\theta \\ \sin^2\theta + i\cos^2\theta \end{bmatrix} && (19) \\
&\propto e^{\frac{-i\pi}{4}} \begin{bmatrix} (1-i)\cos\theta\sin\theta \\ 0 \end{bmatrix} && (20)
\end{aligned}$$

The maximum transmitted intensity will occur when the squared magnitude of the vector in (19) is maximum, that is, at the maximum of the function

$$f(\theta) = 2\cos^2\theta\sin^2\theta \tag{21}$$

which occurs when $\theta = -45°$ or $\theta = 135°$. Substituting either of these angles into the vector in (19), and multiplying by $e^{-\frac{i\pi}{4}}$, gives

$$\begin{bmatrix} E_{t_x} \\ E_{t_y} \end{bmatrix} \propto \frac{1}{\sqrt{2}} \begin{bmatrix} 1 & 0 \\ 0 & 0 \end{bmatrix} \begin{bmatrix} i \\ 1 \end{bmatrix} \tag{22}$$

and thus the light emerging from the quarter wave plate is circularly polarized. If we now rotate the analyzer such that its transmission axis forms and angle ϕ with the horizontal axis of the optical system, (22) becomes

$$\begin{aligned}
\begin{bmatrix} E_{t_x} \\ E_{t_y} \end{bmatrix} &\propto \frac{1}{\sqrt{2}} \begin{bmatrix} \cos^2\phi & \sin\phi\cos\phi \\ \sin\phi\cos\phi & \sin^2\phi \end{bmatrix} \begin{bmatrix} i \\ 1 \end{bmatrix} && (23) \\
&\propto \frac{1}{\sqrt{2}} \begin{bmatrix} i\cos^2\phi + \sin\phi\cos\phi \\ i\sin\phi\cos\phi + \sin^2\phi \end{bmatrix} && (24)
\end{aligned}$$

The squared magnitude of the vector in (24) is a constant, which implies that rotating the analyzer should have no effect on the intensity of the transmitted light.

The second setup of the experiment is designed in order to find the phase shift ϕ due to an overhead transparency. The new setup makes the beam pass through a vertical linear polarizer, the overhead transparency with its fast axis set at an angle of θ with respect to the transmission axis of the polarizer, a quarter wave plate with its fast axis at an angle of ψ with respect to the fast axis of the transparency, and an analyzer with its transmission axis at an angle of ϑ with respect to the fast axis of the quarter

wave plate. The angles ψ and θ have to be chosen such that the transmission of the compound optical system is zero. This gives the matrix equation

$$\left(R(-\theta-\psi-\vartheta)\begin{bmatrix}1&0\\0&0\end{bmatrix}R(\theta+\psi+\vartheta)\right)\left(R(-\theta-\psi)\begin{bmatrix}1&0\\0&i\end{bmatrix}R(\theta+\psi)\right)$$
$$\left(R(-\theta)\begin{bmatrix}1&0\\0&e^{i\phi}\end{bmatrix}R(\theta)\right)\begin{bmatrix}0\\1\end{bmatrix} = \begin{bmatrix}0\\0\end{bmatrix} \quad (25)$$

where $R(\alpha)$ corresponds to the rotation matrix

$$R(\alpha)=\begin{bmatrix}\cos\alpha & \sin\alpha\\ -\sin\alpha & \cos\alpha\end{bmatrix} \quad (26)$$

A very lengthy application of matrix and trigonometric algebra leads to the relationship

$$\tan\phi=-\frac{\tan 2\vartheta}{\sin 2\psi} \quad (27)$$

from which it follows that ϕ is independent of the transparency angle θ.

3 Experimental Set-Up and Results

3.1 Preliminary observations

Before performing the experiments, a series of preliminary exercises using polarizers and calcite crystals were carried out. First, we went outdoors and looked at a point in the sky close to orthogonal with respect to the sun's rays and observed what happened to the transmitted brightness of light through a polarizer as we rotated the polarizer in front of us. We observed that the brightness fluctuated from minimum to maximum as we rotated the polarizer by 90°. This is evidence that the light coming from that point in the sky is partially polarized, because of the phenomenon described in section 2.5.

The second preliminary exercise involved looking at a printed page, first through a calcite crystal, and second through a polarizer and a calcite crystal. Looking at the page through the crystal alone resulted in a double image of the printed letters, which results from the fact that the crystal is an example of a birefringent material. Once the polaroid is inserted between the crystal and the eye, we observed that rotating it resulted in the double images appearing and disappearing, and the relative brightness of each of the images changing. This is consistent with the nature of birefringence and the polarizing effect of the polaroid, as the crystal gives the light from the page an elliptical polarization, which is then converted to linear to varying degrees by the polarizer, depending on the polarizer's orientation and the crystal's thickness.

Finally, we crossed a polarizer and an analyzer and inserted a sheet of mica in between them. The light transmitted with the mica present was brighter than that without the mica, and was separated into different colors, illustrating the birefringent properties of the sheet, and the fact that the incident light on the first polarizer is natural light of different frequencies. Rotating one of the polarizers resulted in the light becoming brighter and whiter, and continued rotation resulted in the transmitted light having the same characteristics as before. This occurs because the angle between the transmission axis of the polarizer and the optic axis of the mica sheet varies, and thus the polarizer blocks different components of the light emerging from the mica.

3.2 Experiment 1

3.2.1 Set-Up

We mount a laser and place polarizer in front of it. We then measure the intensity I_0 transmitted by this polarizer using a photosensor placed directly after it. We proceed to observe how I_0varies as a function of the the polarizer angle θ_p read off its rotation stage. Next, we place a second polarizer, the analyzer, in between the first polarizer and the photosensor, and rotate it, measuring the transmitted intensity as a function of its angle of rotation θ_a, as given by its rotation stage. We use these measurements to test Malus's Law and to find the extinction ratio of the system, $\frac{I_{min}}{I_{max}}$.

3.2.2 Results and analysis

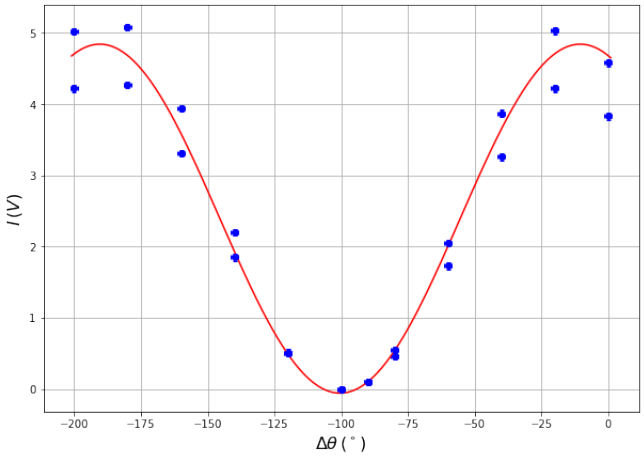

Figure 1: I vs$\Delta\theta$, for the case where $\theta_p = 0 \pm 1°$. The data points are in blue and the line in red represents the best fits for the parameters of the model given in (27).

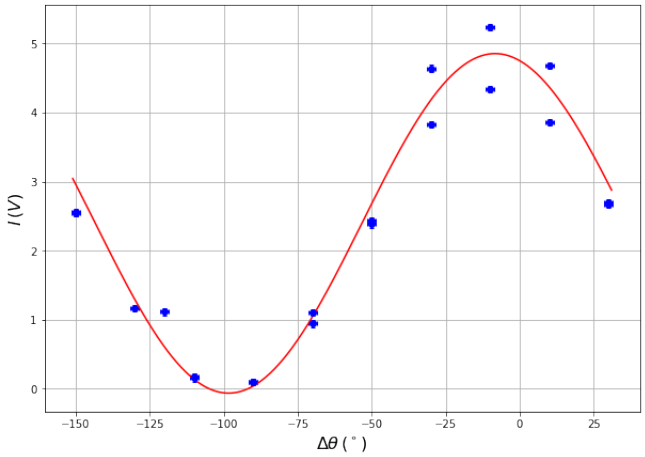

Figure 2: I vs$\Delta\theta$, for the case where $\theta_p = 30 \pm 1°$. The data points are in blue and the line in red represents the best fits for the parameters of the model given in (28).

We measured the intensity as a function of θ_a, for two different values of the angle of the polarizer θ_p, $0° \pm 1°$ and $30° \pm 1°$. The experiment was particularly complicated given that the intensity of the transmitted beam fluctuated considerably over variable periods of time between a minimum and maximum value once a polarizer was put in front of it. We attempted to measure the values at the maxima and minima of each fluctuation for a given θ_a, but we decided not to use the measured value of I_0 since the amplitude of the fluctuations was too large for the case of a single polarizer, and because this amplitude varied as a function of θ_p. Instead, we fit a model given by

$$I(I_0,\, \theta_p,\, \theta_a,\, I_{min}) = I_0 \cos^2(\theta_p - \theta_a + \phi) + I_{min} \tag{28}$$

and plot both the minimum and maximum values of the intensity as a function of $\Delta\theta = \theta_p - \theta_a$. The parameter ϕ gives us the location of the eigenstates of the analyzer, and allows us to obtain the relationship between the angle measured by the rotation stages $\Delta\theta$ and the real angle between the transmission axes of the polarizers, $\Delta\theta_{real}$,

$$\Delta\theta = \Delta\theta_{real} - \phi \tag{29}$$

Figures 1 and 2 show the results for the cases when $\theta_p = 0 \pm 1°$ and $\theta_p = 30 \pm 1°$. The best value for I_o was found to be $4.91 \pm 0.13\, V$, by averaging the best values for obtained for each of the two cases. Similarly, the best fit value for $\phi = 9.4 \pm 1.1°$. It was not possible to recover an accurate value for the extinction ratio due to the fact that the intensity at the minima was less than the intensity of the ambient light, and as such the errors involved in the calculations became too big. For instance, we measured the intensity of the background lights in the room to be $15 \pm 5\, mV$, and the values recorded by the voltmeter close to the minima were ~20 mV, which included the contribution of the ambient lights. In fact, the optimal fits for I_{min} were negative in both cases, and the magnitude of the average error for the extinction ratio ended up being 7000% greater than the magnitude of its nominal value.

3.3 Experiment 2

3.3.1 Set-Up

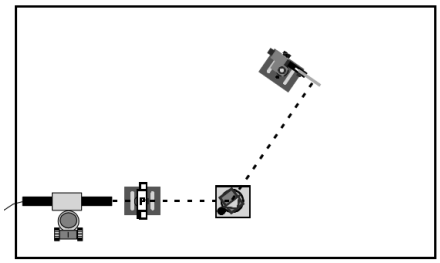

Figure 3: Set-up for experiment 2, obtained from [6].

The objective of this experiment was to find Brewster's angle. Figure 3 shows a diagram of the set-up used. From left to right, the symbols in the figure represent the laser, a polarizer set with its transmission axis parallel to the table, a glass prism mounted atop a pedestal on a rotation stage, and a beam stopper. Brewster's angle was determined by measuring the intensity I of the reflected light as a function of the incident angle θ_i, and finding the minima in the resulting curve.

3.3.2 Results and analysis

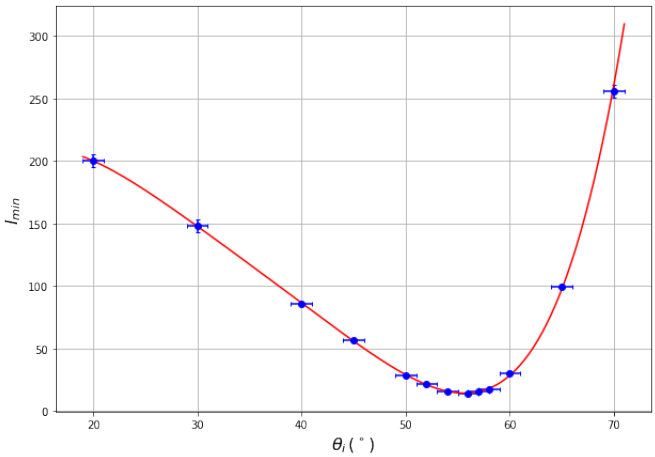

Figure 4: I_{min} vs θ_i. The data points are in blue and the line in red represents the best fits for the parameters of the model given in (31).

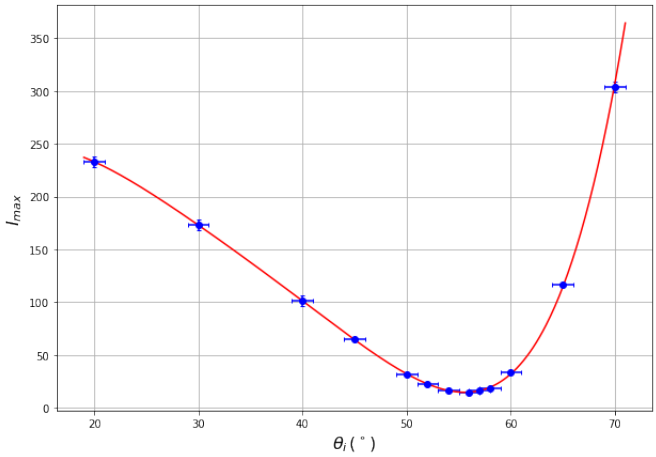

Figure 5: I_{max} vs θ_i. The data points are in blue and the line in red represents the best fits for the parameters of the model given in (30).

Again, to account for the fluctuations of the laser, we measured both the minimum and maximum values of the intensity, I_{min} and I_{max}at each angle of incidence. The results of these measurements are shown in Figures 4 and 5. We model the observed curve in terms of a quintic polynomial with equation

$$f(\theta_i,\, a,\, b,\, c,\, d,\, e,\, f) = a\theta_i^5 + b\theta_i^4 + c\theta_i^3 + d\theta_i^2 + e\theta_i + f \tag{30}$$

The minimum occurs at one of the four roots of the quartic equation given by

$$5a\theta_i^4 + 4b\theta_i^3 + 3c\theta_i^2 + 2d\theta_i + e = 0 \tag{31}$$

which can be found by applying the elementary formulae for the roots of a quartic equation. We find that for both cases, the minimum occurs at $\theta_B = 55.6 \pm 1.0°$, giving a refractive index of $n = 1.46 \pm 0.05$. This is consistent with the values found, with the nominal value within 4% of the value given by the manufacturer of $n = 1.517$ (as given in [6]), and almost within the error bars. However, this measurement of the refraction index is not as accurate as those performed in the previous project, where the discrepancies were never greater than 2%, and were as low as 0.2%. The reason for this likely resides in the alignment of the reflecting interface of the prism with respect to the incident light. This was done by having the light reflected from the prism in the initial position to go back into the laser aperture. However, even a very small angle of deviation from perfect alignment gives rise to significant errors. For instance, if this misalignment was on the order of 0.5° in the appropiate direction, the minimum occurs at $56.1 \pm 1°$ instead of $55.6 \pm 1°$, and the nominal value of the refractive index increases to $n = 1.49$, which is much closer to the desired value. Reducing this error can be achieved by means of placing the prism farther away from the laser, so as to make any deviation in alignment more noticeable to the naked eye.

3.4 Experiment 3

3.4.1 Set-Up

First, we mount a polarizer in front of the laser and measure the intensity of light polarized parallel to the plane of incidence $I_{\|_i}$ and the intensity of light polarized perpendicular to the plane of incidence

$I_{\perp_i}$. Then, the set-up becomes identical to that of experiment 2, except for the fact that a blackened flat is used instead of the glass prism. This flat was blackened in order to decrease the amount of light reflected. We then proceed to measure the intensity of the reflected light as a function of θ_i for parallel incident polarization $\left(I_{\parallel_r}\right)$ and perpendicular incident polarization $(I_{\perp_i})$. Finally, we orient the polarizer with its transmission axis at an angle of 45° with respect to the plane of incidence, and mount an analyzer on a rotation stage in front of the reflected beam. We look for the angle ψ of the analyzer with respect to the plane of incidence that results in the extinction of the transmitted light, thus enabling us to measure the orientation of the reflected polarization. The components of the electric field then should satisfy $\tan\psi = \frac{E_\parallel}{E_\perp}$. We measure ψ for different θ_i.

3.4.2 Results and analysis

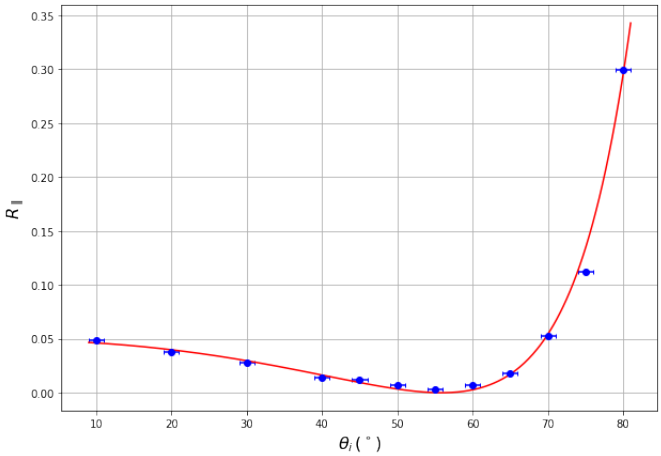

Figure 6: $R_\parallel$ vs θ_i. The data points are in blue and the line in red represents the best fits for the parameters of the model given in (32).

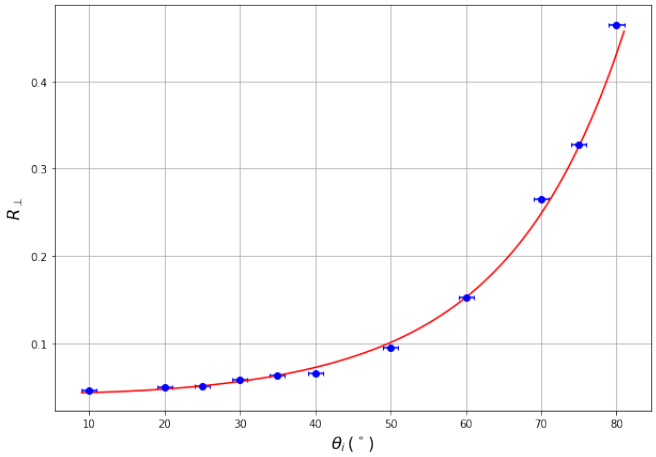

Figure 7: $R_\perp$ vs θ_i. The data points are in blue and the line in red represents the best fits for the parameters of the model given in (33).

We first plot $\frac{I_{\parallel_r}}{I_{\parallel_i}} = R_\parallel$ and $\frac{I_{\perp_r}}{I_{\perp_i}} = R_\perp$ as a function of θ_i and fit using two different models, given by

$$f\left(\theta_i,\, \phi_\parallel,\, n_\parallel\right) = \left(\frac{n_\parallel^2 \cos\left(\theta_i + \phi_\parallel\right) - \sqrt{n_\parallel^2 - \sin^2\left(\theta_i + \phi_\parallel\right)}}{n_\parallel^2 \cos\left(\theta_i + \phi_\perp\right) + \sqrt{n_\parallel^2 - \sin^2\left(\theta_i + \phi_\perp\right)}}\right)^2 \tag{32}$$

$$g\left(\theta_i,\, \phi_\perp,\, n_\perp\right) = \left(\frac{\cos\left(\theta_i + \phi_\parallel\right) - \sqrt{n_\perp^2 - \sin^2\left(\theta_i + \phi_\parallel\right)}}{\cos\left(\theta_i + \phi_\perp\right) + \sqrt{n_\perp^2 - \sin^2\left(\theta_i + \phi_\perp\right)}}\right)^2 \tag{33}$$

which follows from section 2.7, but where we have also introduced parallel and perpendicular phase offsets to correct for possible deviations from perfect alignment, in terms of the horizontal and vertical orientations of the flat with respect to the incident plane, and the adjustment of the polarizer using Brewster's angle. The results are shown in Figures 6 and 7. We find that $n_\parallel = 1.57 \pm 0.01$, $\phi_\parallel = 1.6 \pm 0.5°$, $n_\perp = 1.52 \pm 0.01$, and $\phi_\perp = -4.1 \pm 0.7°$. These results are consistent with Fresnel's equations and indicate that the system alignment was performed reasonably well, given the small value of $\phi_\parallel$ and $\phi_\perp$. The ~3% discrepancy in the values for the refractive index can be explained by measurement errors in the reflected intensity, due to the intensity fluctuations from the laser. This was not included in the value of the uncertainty related to each of the measurements because it was very hard to quantify, but since we only measured the values at the fluctuation maxima, performing similar measurements at the minima would certainly increase the error bars such that both values of the refractive index overlap. A more detailed analysis of this effect could in principle be performed by studying the fluctuations directly, but this was not done due to time constraints.

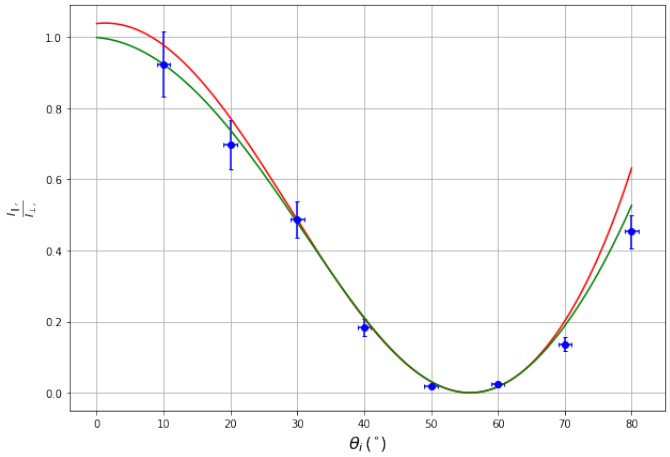

Figure 8: $\frac{I_{\perp_i}}{I_{\parallel_i}} \tan^2 \psi$ vs θ_i. The data points are in blue. The line in red represents the fit using a combination of the models from (32) and (33), whereas the green line arises from the fit using (34).

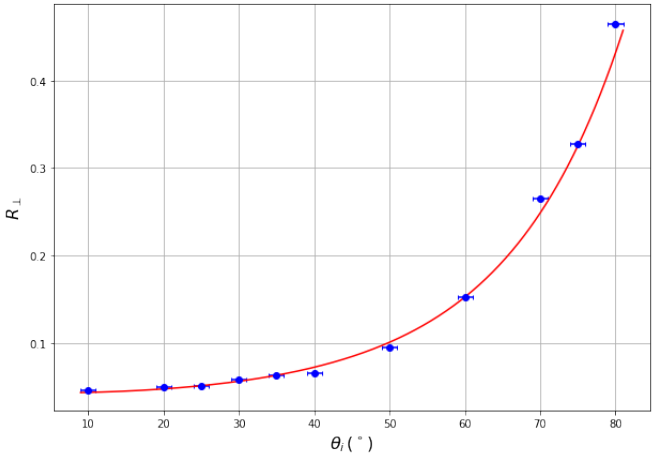

Figure 9: $R_\perp$ vs θ_i. The data points are in blue and the line in red represents the best fits for the parameters of the model given in (33).

The relationship between the azimuthal angle and the amplitude of the electric field components implies that

$$\tan^2 \psi = \frac{I_{\parallel_r}}{I_{\perp_r}} = \left(\frac{-1 + \cos 2\theta_i + 2\cos\theta_i \sqrt{n^2 - \sin^2 \theta_i}}{-1 + \cos 2\theta_i - 2\cos\theta_i \sqrt{n^2 - \sin^2 \theta_i}} \right)^2 \frac{I_{\parallel_i}}{I_{\perp_i}} \tag{34}$$

To determine the agreement between these two methods of verifying Fresnel's equations, we fit a model according to (34), but again we add an offset ϕ such that $\theta_i \to \theta_i + \phi$, to minimize any possible errors in the alignment, and find the best fit for n. We find that the best fit value for n in this case is

$n = 1.40 \pm 0.1$, which is significantly lower than the values found for n from the reflection coefficients. An illustration of how the two models differ is given in Figure 8, where we use both models to fit for the values of $\frac{I_{\parallel r}}{I_{\perp r}}$ as calculated from the measurements of ψ. We see that the model in (34) gives a better fit than the combination of models in (32) and (33). The differences arise because the models in (32) and (33) attempt to measure the reflection coefficients directly, and test the Fresnel equations by setting n as a free parameter. Comparing the two values of n obtained give us a good idea of how well the Fresnel equations hold. Setting n as a free parameter, however, implies that the ratio $\frac{I_{\parallel r}}{I_{\perp r}}$ calculated from such a model can potentially be more than unity. The model in (34), on the other hand, uses a single value for n, which means that the ratio's maximum value never exceeds one, and since the tangent of any angle is never larger than one, this model provides a better fit for the ratio as a function of θ_i arising from the measurement of the azimuthal angle.

The minimum value of the plot corresponds to Brewster's angle. We have not plotted $\tan\psi$ vs θ_i, but doing so would have shown that the ratio between the components of the electric field intercepts the x-axis at Brewster's angle, and proceeds to become negative, because crossing this angle introduces a phase shift of 90° between the components. The reason why this cannot be observed by measuring the intensities directly is that these correspond to the square of the electric field components.

3.5 Experiment 4

3.5.1 Set-Up

We place a vial filled with water and a small amount of skim milk in front of the laser, and qualitatively observe the characteristics of the scattered light with respect to the angle of observation. We then place a polarizer in between the laser and the vial, and observe the scattered light at an angle of 90° with respect to the direction of propagation of the beam as we rotate the polarizer.

3.5.2 Results and analysis

For the case in which the light incident on the vial is unpolarized, we observe that the maximum intensity of the scattered light occurs when looking at the vial from an angle that is directly opposite to the incident laser beam. The reason for this is that no polarization occurs in this direction, since the molecules are not able to oscillate in that axis, which results in no interference between the incident radiation and the light reradiated by the molecules. The minimum intensities occur at angles perpendicular to the direction of propagation, at which points the scattered light is completely plane polarized. This effect becomes more evident once we introduce a polarizer in between the laser and the vial. Observing the vial at 90° angles with respect to the direction of propagation, it is possible to rotate the polarizer into positions that result in no scattered light being observed, something that is not possible to do when looking at the vial from an angle parallel to the direction of propagation. Essentially, then, the system is similar to the one studied in experiment 1, with the extinction ratio depending on the angle of observation.

3.6 Experiment 5

3.6.1 Set-Up

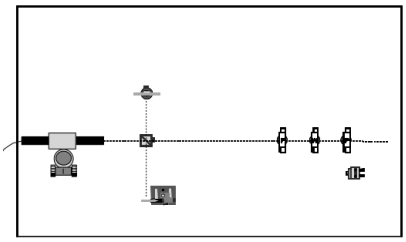

Figure 10: Set-up for the last part of experiment 5, obtained from [6].

We start by placing two polarizers at a distance of 30 cm away from the laser. We proceed to place a quarter wave plate in between the two polarizers. We find the eigenstates of the quarter wave by crossing the two polarizers and finding the orientations of the plate that result in no transmitted intensity. Next, we find the orientations of the quarter wave plate that result in maximally transmitted intensity, which corresponds to the setup in which the quarter wave plate is transmitting circularly polarized light. Then, we rotate the analyzer and look for variations in the intensity of the transmitted light.

We now attempt to measure the phase shift introduced by an overhead transparency, using equation (27). We cross the polarizers and place the overhead transparency in between them. We then find the eigenstates of the overhead transparency by the same method we used to find the eigenstates of the quarter wave plate. We proceed to rotate the transparency by $45°$ with respect to the position of one of its eigenstates, and place the quarter wave plate in between the transparency and the analyzer. We now rotate the quarter wave plate by an angle ψ with respect to the transparency and the analyzer by an angle ϑ with respect to the quarter wave plate, such that no light is transmitted by the analyzer. We repeat this procedure for different orientations of the transparency.

Finally, we build an optical isolator by adjusting the quarter wave plate such that it gives off circularly polarized light, following the procedure described above. We now replace the analyzer with a mirror and qualitatively measure the intensity of the reflected light that passes through the quarter wave plate and the polarizer in the opposite direction, by placing a beam splitter in between the laser and the polarizer and placing a beam stopper at 90^0 with respect to the laser and the beam stopper, as shown in Figure 10.

$\theta_t\,(^\circ)(\pm 1^\circ)$	$\theta_{qw}\,(^\circ)(\pm 1^\circ)$	$\theta_a\,(^\circ)(\pm 1^\circ)$	$\phi\,(^\circ)$	$\Delta\phi\,(^\circ)$
107	200	100	81	4
120	210	90	64	20
130	215	85	64	30
140	223	85	73	10

Table 1: Measurements made in order to calculate the transparency retardation ϕ and their individual outcomes.

3.6.2 Results and analysis

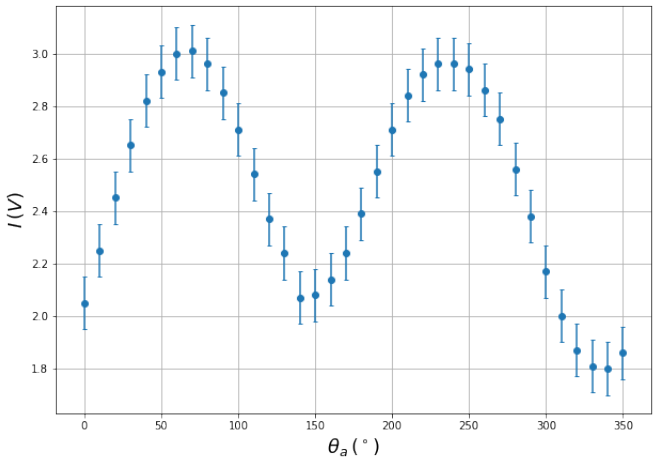

Figure 11: Intensity of transmitted light I vs analyzer angle θ_a.

Rotating the analyzer after following the procedure described above in order to produce circularly polarized light using the polarizer and the quarter wave plate did not produce the expected results. Figure 11 shows the results of plotting the intensity of the transmitted light I as a function of the analyzer angle θ_a. Instead of a straight line, we get an oscillation that looks like a sinusoid plus an offset, although the symmetry is progressively lost due to the intensity fluctuations that we have encountered before. This means that the procedure did not effectively produce circularly polarized light, and instead resulted in elliptically polarized light. The reasons for this are unclear. The results are so far from the expectation that I should not be a function of θ_a, that it is hard to develop a convincing explanation for the phenomenon. We repeated the procedure in the construction of the optical isolator later, and that procedure worked as expected, so we likely committed a significant execution error in this particular attempt.

We measured the retardation introduced by the overhead transparency using the following reasoning. Equation (27) relates ψ and ϑ to the retardation ϕ, but these angles are not possible to measure directly. Instead, they are given by

$$\begin{aligned} \psi &= \theta_{qw} - \theta_t \\ \vartheta &= \theta_a - \theta_{qw} \end{aligned} \tag{35}$$

where θ_{qw} and θ_t correspond to the angles between the fast axes of the quarter wave and the transparency with respect to the horizontal axis of the optical system, and θ_a corresponds to the the angle between the transmission axis of the analyzer and the horizontal axis of the system, which is defined as parallel to the transmission axis of the polarizer. We cannot measure these angles directly either, however, since the rotation stages of the optical elements do not necessarily align with the axes of the respective element. Instead, we find these angles via their relationship with their lowest eigenstate. Let α_{qw}, α_t, and α_a be the lowest eigenstates of the elements as measured by the rotation stage, and let β_{qw}, β_t, and β_a be the angle of each element according to the rotation stage reading, and we have that

$$\begin{aligned} \theta_{qw} &= \beta_{qw} + \alpha_{qw} \\ \theta_t &= \beta_t + \alpha_t \\ \theta_a &= \beta_a + \alpha_a - 90^\circ \end{aligned} \tag{36}$$

It should be obvious from this that the errors involved in the measurement of the retardation are rather large, due to the propagation of error. We performed four measurements, which are tabulated in Table 1. Combining them gives a value for the phase shift$\phi = 70 \pm 10^\circ$. It must be stressed that this result is unreliable not only because of the error propagation: we also found it impossible to actually achieve complete extinction by performing the described procedure, which implies that the RHS of (25) was never actually equal to zero, which in turn means that (27) does not apply exactly, and a dependence on the angle of the transparency with respect to the axes of the system is introduced. A more detailed examination of this is outside the scope of this work, and as such will not be pursued here.

Our attempt to build an optical isolator was successful. Following the procedure described above enabled us to build a system into which light enters but doesn't come out, which we were able to confirm because the beam spot was not visible at the beam stopper. The reason why this works is the following. Once we set up the polarizer and the quarter wave in such a way that the plate transmits circularly polarized light, the light reflected by the mirror is unable to pass through the polarizer because the mirror changes the handedness of the circularly polarized beam, which is linearly polarized in a plane perpendicular to the transmission axis of the polarizer once it passes back through the quarter wave. Thus, a single polarizer is able to act like a combination of two crossed polarizers.

4 Conclusions

We have performed a series of experiments that illustrate the transverse wave nature of light via an examination of its polarizing properties. Most, but not all, of our results have agreed with expectations. Better results would probably be obtained with the modification of two things in particular. First, it would have been much easier to conduct the experiments using a laser whose beam's intensity did not fluctuate as much as ours once it was passed through one or more polarizers. As mentioned above, these fluctuations potentially led to significant errors. The other significant source of error in most of the experiments performed was the precision of the scale in the rotation stages. Using rotation stages of larger radii would be very useful especially in procedures like the one used to determine the retardation of the overhead transparency, where the relatively low precision of this scale resulted in large final errors once the errors of each of the measurements were combined. Larger rotation scales would also have been useful for measuring Brewster's angle.

5 Acknowledgements

The author of this work would like to acknowledge the help received from his lab partner, Juliette Fropier, throughout the data gathering process. I was unable to attend one of the lab sessions, and she competently performed part of the project by herself, and allowed me to used her data, so I am particularly grateful for that. I would also like to acknowledge the help provided by our TA, David Moreau, during lab time.

References

[1] Jones E, Oliphant E, Peterson P, et al. *SciPy: Open Source Scientific Tools for Python,* 2001-, http://www.scipy.org/.

[2] Lebigot, E.O. *Uncertainties: a Python package for calculations with uncertainties*, http://pythonhosted.org/uncertainties/

[3] Griffiths, D. J. *Introduction to Electrodynamics, 4th edit.*, Pearson Education Inc. 2013.

[4] Born, M. & Wolf, E. *Principles of Optics, 7th (expanded) edit.,* Cambridge University Press, 1999.

[5] Hecht, E. *Optics*, *5th edit.*, Pearson Education Limited 2017.

[6] Bodenschatz, E., et al. *Modern Experimental Optics Laboratory Manual*, Cornell University Physics Department 2016.